Study of a Polymeric Network by Dynamic Fluorescence Quenching Using a Blob Model

Veena Vangani and Jean Duhamel*

Institute for Polymer Research, Department of Chemistry, University of Waterloo, Waterloo, Ontario N2L 3G1, Canada

Sandor Nemeth and Tze-Chi Jao

Ethyl Research Center, Richmond, Virginia 23219

Received July 16, 1998; Revised Manuscript Received February 3, 1999

ABSTRACT: The association behavior of a maleic anhydride grafted and pyrene labeled ethylene−propylene random copolymer was studied using fluorescence spectroscopy. The labeling was achieved with 1-pyrenebutanoic acid hydrazide via the grafted anhydride groups. The resulting polar grafts induced intra- and intermolecular associations among the polymer chains in apolar solvents. This association process was studied using steady-state and time-resolved fluorescence spectroscopy as a function of polymer concentration. Due to the high complexity of the polymer system, an improved approach of handling the time-resolved fluorescence data had to be introduced. Thus, the quantitative analysis of the fluorescence decays was carried out using a novel model in which the polymer network is divided into blobs among which the chromophores distribute themselves randomly, according to a Poisson distribution. Results show that, as the polymer concentration is increased, the number of polar group aggregates increases. However, the local concentration of aggregated polar groups in the polymer network does not change. This indicates that as polymer concentration is increased, either that there are only a few polymer aggregates in the solution that increase in size and keep the concentration of polar junctions constant throughout the polymeric network or that more polymer aggregates are formed. This latter process would be reminiscent of micelle formation. This behavior is observed until the overlap concentration ($c^* = 10-20$ g/L), above which newly formed polar aggregates contribute to increasing the local aggregate concentration.

Introduction

Associating polymers (AP) are polymers, normally soluble in a given solvent, onto which small insoluble units have been grafted. These insoluble moieties associate[1] in solution, leading to the formation of large polymer aggregates.[1a,2] The peculiar ability of AP to form transient aggregates has made them useful in many practical applications such as thickeners in paint, drag reducing agents in pipelines, colloid stabilizers in oil and paint, and oil recovery enhancers.[3]

Ethylene−propylene (EP) copolymers are extensively used in the petroleum industry as additives for motor oil. When grafted with polar functional groups, such as maleic anhydride, they interact with colloidal matter in oil, hence acting as dispersants. These polymers associate in an apolar solvent via their polar moieties and sufficiently long polyethylene sequences which form small intermolecular ordered domains.[1a] In hexane, for example, these AP form a polymeric network that is held together, in part, by the polar aggregates.[1a,4] Our work aims at better understanding the nature of these associations and their effects on the polymer chain dynamics by studying an EP random copolymer grafted with the polar maleic anhydride.

Fluorescence spectroscopy is a very powerful tool for monitoring polymer chain dynamics,[5] and it was used to study an oil-soluble AP. However, it required appropriate fluorescent molecules. Thus, a pyrene chromophore was attached to the anhydride groups by reacting the grafted EP copolymer with 1-pyrenebutanoic acid hydrazide. Since the polar groups are labeled with the pyrene chromophore, the polar aggregates induce the formation of pyrene aggregates.

However, not all pyrene groups are involved into polar aggregates. The unassociated pyrene groups can undergo diffusional motion. Upon photon absorption, an excited pyrene might either fluoresce or encounter a ground-state (GS) pyrene via diffusion and form an excimer. Monitoring the rate of disappearance of the excited pyrene as well as the rate of excimer formation yields insightful dynamical information about the polymer, since excimer formation requires the encounter of two monomeric units of the polymer carrying the pyrene chromophore.

Although potentially informative, this fluorescence approach is limited to simple polymeric systems in solution. The rate of excimer formation is greatly affected by the polymer length separating two chromophores.[5] Consequently, quantitative time-resolved fluorescence studies of pyrene labeled polymers require that the chromophores be located at specific positions of well-characterized polymers (usually at the chain ends of a monodisperse polymer) so that existing models can be applied, based typically on the Birks' scheme.[6] The pyrene labeled EP copolymer that we investigated clearly does not fit into this category. It is polydisperse in length ($M_w/M_n = 1.6$), and the pyrene groups are randomly attached onto the backbone, inducing a distribution of excimer formation rates.

To further complicate this polymeric system, polar aggregation between the polar maleic anhydride moieties takes place in apolar solvents, which results in the

* To whom correspondence should be addressed.

10.1021/ma981129k CCC: $18.00
Published on Web 04/13/1999

Scheme 1

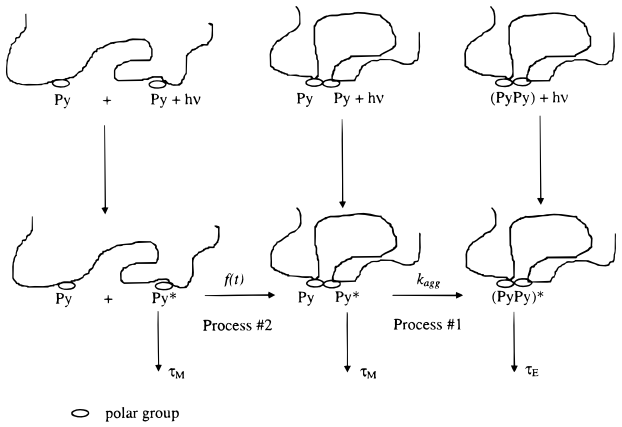

formation of pyrene aggregates.[1a,4] Two pyrene populations are present in solution: (a) the pyrene associated into aggregates via polar interactions and (b) the nonassociated single pyrenes. Consequently, two excimer formation processes must be invoked. They are illustrated in Scheme 1 and are inspired by a model developed by Char et al. for water-soluble AP.[7] In process 1, an excimer is formed between two pyrenes—both located inside a polar aggregate. Process 1 is rapid. In process 2, a single pyrene diffuses through the polymeric network, associates via polar interaction with either another single, nonassociated pyrene or a pyrene aggregate, and forms an excimer according to process 1. Process 2 is slow.

We have carried out a fluorescence study of the pyrene labeled EP copolymer in hexane for polymer concentrations ranging from 0.006 up to 178 g/L. At the low polymer concentrations studied, polar interactions occur mostly intramolecularly but become intermolecular as the polymer concentration is increased.[1a] These polar aggregates bridge several polymer chains together. Upon increasing polymer concentration, our fluorescence data indicate that the local concentration of polar junctions remains constant inside the polymer network. As the polymer concentration further increases, the overlap concentration c^* is reached at about 10−20 g/L, and for polymer concentrations larger than c^*, the density of polar junctions within the network increases.

We quantitatively interpret our fluorescence decay measurements with a model where the polymer network is divided into blobs, and the pyrene groups partition themselves randomly into the blobs following a Poisson distribution.[8] To our knowledge, it is the first time that this type of quantitative analysis is carried out for a system presenting such a high level of polydispersity: The polymer chains are polydisperse in length ($M_w/M_n = 1.6$), the polymer aggregates are polydisperse in size, and the distance between two labels are polydisperse as well, due to the random pyrene labeling of the polymer. The inherent polydispersity of the system makes it somewhat difficult to apply the global compartmental analysis method which has been developed so far for well-characterized systems.[9]

Experimental Section

Polymer Labeling, Purification, and Characterization. The EP random copolymer grafted with maleic anhydride and labeled with pyrene was provided to us by Ethyl Corp. This polymer contained 60 mol % of ethylene and 9×10^{-5} mol of pyrene per gram of EP copolymer. The grafting and pyrene labeling procedures have been described elsewhere.[4] According to these procedures, a second EP copolymer containing 60 mol % of ethylene was modified and labeled with pyrene so that it contained 5×10^{-5} mol of pyrene per gram of polymer. This second copolymer was used *uniquely* to determine the lifetime of unquenched pyrene attached onto the polymer backbone. The pyrene labeled polymer was purified by dissolution in hexane and reprecipitation in acetone to remove the lower molecular weight impurities (essentially oligomers of maleic anhydride and unreacted dye). This was done five or six times until the pure product was obtained, as confirmed by size exclusion chromatography (SEC) analysis in THF, using a UV detector to monitor the presence of unattached dye. The polymer exhibited a single broad peak in the SEC trace with an estimated M_n of 25 000 and PDI = 1.6, based on a calibration of the SEC system using polystyrene standards.

Materials. Hexane (Glass-Distilled, BDH Inc., Canada), THF (HPLC grade, VWR, Canada), and acetone (reagent, Caledon Laboratories Ltd.,Canada) were used as received. 1-Pyrenemethanol (Aldrich, Canada) was crystallized two to three times. 1-Pyrenebutanoic acid hydrazide (Molecular Probes, USA) was used as received.

Size Exclusion Chromatography. The samples were analyzed with a Waters SEC system using THF as an eluent and a Jordi linear DVB mixed bed column. The instrument was coupled with DRI and UV detectors. The absorption wavelength was fixed at 254 nm. The column was calibrated using known molecular weight polystyrene standards. These experiments were carried out at room temperature.

UV Absorption Measurements. A Hewlett-Packard 8452A diode array spectrophotometer was used for the absorption measurements.

Pyrene Content of Polymer Samples. First, the pyrene content of the polymer was established by measuring the absorption of a solution prepared from a carefully weighed amount (m) of pyrene labeled polymer in a known volume of THF (V). THF was chosen because interactions between polar groups are small in this solvent, and pyrene aggregation is limited. Consequently, the absorption spectra are expected not to be distorted. The pyrene concentration [Py] was then estimated from the absorption value at 344 nm and the extinction coefficient of a pyrene model compound, typically 1-pyrenemethanol (ϵ [344 nm, in THF] = 42 700, measured in the laboratory). The pyrene content λ of the polymer could be calculated from $\lambda = [\mathrm{Py}]/(m/V)$ expressed in moles of pyrene per gram of polymer. For these polymers, λ was found to equal 5×10^{-5} and 9×10^{-5} mol g^{-1}.

The presence of pyrene aggregates in hexane distorts the absorption spectra.[10] Thus, concentrations of the polymer in hexane were calculated by introducing a known amount of hexane solution in a separate flask, followed by the evaporation of hexane under a constant flow of nitrogen. The dry polymer was redissolved into a known amount of THF. An absorption spectrum was taken yielding the pyrene concentration. The corresponding polymer concentration was deduced from the value of λ.

Intrinsic Viscosity Measurements. Viscosity measurements were made with an Ubbelohde viscometer in a water bath at 25 ± 0.1 °C. For these measurements, polymer concentrations ranged from 4 to 15 g/L.

Steady-State Fluorescence Measurements. They were carried out on a Photon Technology International LS-100 steady-state system with a pulsed xenon flash lamp as the light source. Fluorescence spectra of Py-EP*g*MA solutions having a concentration above 1 g/L were obtained using the front face geometry. Fluorescence spectra of more dilute solutions were taken with the more usual right angle configuration.

To preferentially excite the pyrene monomer and the GS pyrene aggregates, fluorescence emission spectra were obtained at two excitation wavelengths, 344 and 350 nm, respectively. For the same reasons, fluorescence excitation spectra were obtained at the two emission wavelengths, 377

and 520 nm. The fluorescence intensities of the monomer (I_M) and of the excimer (I_E) were calculated by taking the integrals under the fluorescence spectra from 374 up to 382 nm for the pyrene monomer and from 500 up to 530 nm for the pyrene excimer.

Time-Resolved Fluorescence Spectroscopy. The fluorescence decay profiles were obtained by the time-correlated single photon counting (TCSPC) technique using a Photochemical Research Associates Inc. System 2000 instrument. For all TCSPC experiments, the excitation wavelength was set at 344 nm. The decay curves were obtained by setting the emission wavelength at 377 nm for the monomer and 520 nm for the excimer. To block potential light scattering leaking through the detection system, filters were used with a cutoff at 370 and 495 nm to acquire the fluorescence decays of the pyrene monomer and excimer, respectively. At polymer concentrations lower than 1 g/L, fluorescence decays were collected with a right angle configuration. At higher polymer concentrations, the higher optical densities required a front face arrangement to obtain sufficiently strong fluorescence signal. The decays were collected over 512 channels. The lamp profile was obtained by exciting a Ludox scattering solution at 344 nm and collecting its emission at the same wavelength. A total of 20 000 counts were collected at the peak maximum of the lamp and the decay curves, and the data were then analyzed.

All polymer solutions for the steady-state and lifetime measurements were prepared by dissolving the required polymer amount in hexane and degassing the solutions under a gentle flow of nitrogen for 20 min.

Fluorescence Decay Analysis. A function $g(t)$ was assumed to fit the fluorescence decays. It was convoluted with the instrument response function $L(t)$ to fit the experimental decay $G(t)$[11]

$$G(t) = L(t) \otimes g(t) \tag{1}$$

where the symbol $\otimes$ indicates the convolution performed between the experimental instrument function and the fitting function $g(t)$. The function $g(t)$ was either a sum of exponentials with an expression given in eq 2, where the number of exponentials n is varied from 1 to 4, or the more complicated eq 4 whose meaning is explained in the Discussion section and whose derivation is given in the Appendix. Equation 4 involves a series that was calculated up to the 11th term in our analysis program. According to the experimental parameters that we retrieved from our analysis, the contribution of the higher terms is negligible.

$$g(t) = \sum_{i=1}^{i=n} A_i e^{-t/\tau_i} \tag{2}$$

The parameters of $g(t)$ were retrieved by using a least-squares curve fitting program based on the Marquardt−Levenberg algorithm.[12] The goodness of the fit was assessed from the χ^2 parameter ($\chi^2 < 1.2$ for a good fit) and the random distribution of the residuals and of the autocorrelation function.

Results

The results presented in this work have all been obtained with the Py−EP*g*MA containing 9×10^{-5} mol of pyrene per gram of polymer. The Py−EP*g*MA copolymer containing 5×10^{-5} mol of pyrene per gram of polymer was used *uniquely* to determine the lifetime of unquenched pyrene monomer attached onto the polymer backbone.

The fluorescence spectra of a THF and hexane solution of Py−EP*g*MA are shown in Figure 1a,b. Between 370 and 400 nm, the spectra exhibit the peaks characteristic of the pyrene monomer. Between 450 and 550 nm one recognizes the broad structureless fluorescence

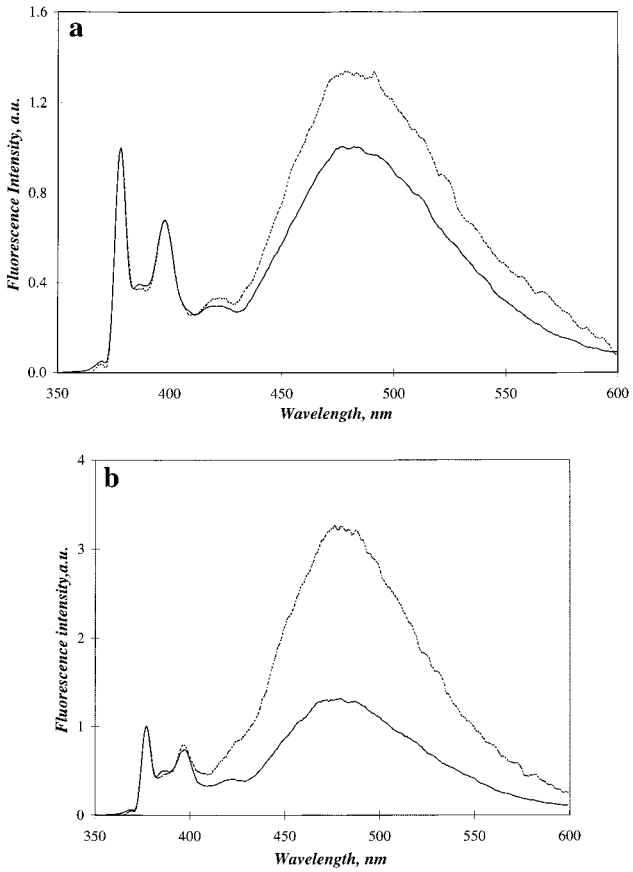

Figure 1. (a) Fluorescence emission spectra of a 0.018 g/L solution of Py−EP*g*MA in THF: (—) $\lambda_{ex} = 344$ nm; (- - -) $\lambda_{ex} = 350$ nm. (b) Fluorescence emission spectra of a 0.030 g/L solution of Py-EP*g*MA in hexane: (—) $\lambda_{ex} = 344$ nm; (- - -) $\lambda_{ex} = 350$ nm.

emission of the pyrene excimer. Excitation spectra were obtained by fixing the emission wavelength at 377 and 500 nm. Were no GS pyrene aggregates present, the two spectra should overlap. This is observed in THF (Figure 2a), a polar solvent, but not in hexane (Figure 2b), an apolar solvent, where the two spectra exhibit a clear shift, evidence of the presence of GS pyrene aggregates.[10] Because the fluorescence emission of the pyrene monomer dominates at 377 nm, the excitation spectrum obtained by fixing the emission wavelength at 377 nm is characteristic of the pyrene monomer. Since GS pyrene aggregates bring together at least two pyrene chromophores in a small volume, they readily form excimers, and their contribution is expected to appear mainly in the excimer fluorescence band. The shifted excitation spectrum obtained with a fixed emission wavelength of 500 nm is thus indicative of the presence of the GS pyrene aggregates. Since this shift is much less pronounced in more polar THF, it implies that polar interactions are bringing the pyrene groups close to each other.[1a,4]

Figure 2b shows that a large difference in the fluorescence intensities is observed when using 350 nm excitation. On the other hand, the fluorescence intensities observed when using 344 nm excitation have much closer values. Consequently, exciting the Py−EP*g*MA at 350 nm should yield a much larger ratio of excimer relative to monomer (I_E/I_M[350]), than would be observed in the same solution when it is excited at 344 nm (I_E/I_M[344]), where both populations (unassociated pyrene and GS pyrene aggregates) contribute more

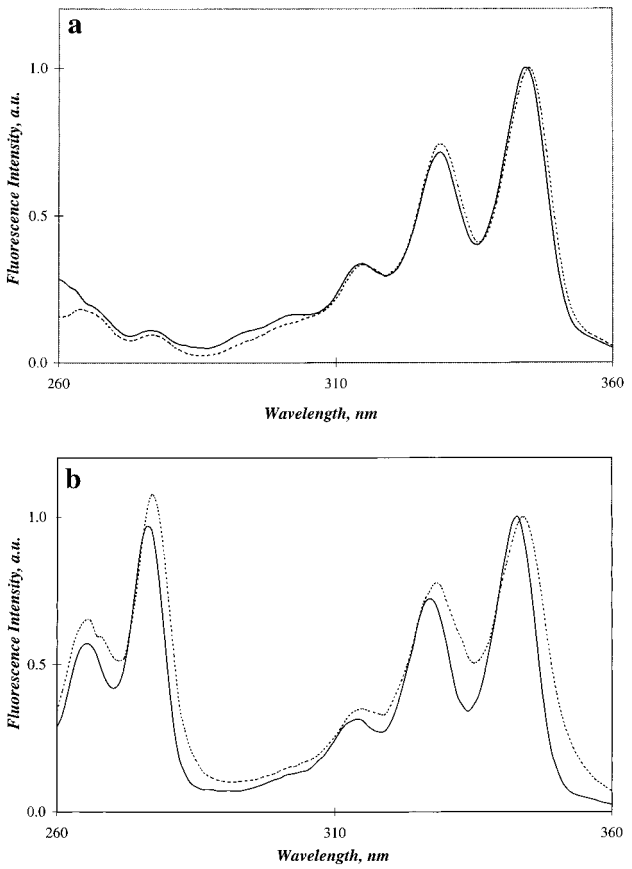

Figure 2. (a) Fluorescence excitation spectra of a 0.018 g/L of Py-EP*g*MA in THF: (—) $\lambda_{em} = 377$ nm; (- - -) $\lambda_{em} = 500$ nm. (b) Fluorescence excitation spectra of a 0.030 g/L of Py-EP*g*MA in hexane: (—) $\lambda_{em} = 377$ nm; (- - -) $\lambda_{em} = 500$ nm.

evenly. GS pyrene aggregates can be excited preferentially at 350 nm to form excimer readily. This effect is indeed observed and is shown in Figure 1b where the ratio $\{I_E/I_M[350]\}/\{I_E/I_M[344]\}$ equals 2.5. For all polymer concentrations that were studied in hexane, the ratios I_E/I_M obtained after excitation at 350 nm were always larger than those obtained with the same solutions excited at 344 nm. This demonstrates the presence of pyrene aggregates at all polymer concentrations.

In THF where the excitation spectra exhibit a much better overlap (cf. Figure 2a), Figure 1a yields a ratio $\{I_E/I_M[350]\}/\{I_E/I_M[344]\}$ equal to 1.3. Since this ratio is much closer to 1.0 in THF than in hexane, it indicates that GS pyrene aggregates are present to a much lesser extent in more polar THF than in hexane.

The fluorescence behavior of the polymer solutions was monitored for polymer concentrations ranging from 0.006 up to 10 g/L for steady-state fluorescence measurements and from 0.006 up to 178 g/L for time-resolved fluorescence measurements. At the lowest polymer concentrations, polar associations are expected to occur mostly intramolecularly.[1a] As more polymer molecules are added to the solution, intermolecular associations are generated.[1a] They signal the onset of the formation of a polymer network held together via intermolecular polyethylene crystallites and polar aggregates. This process triggers a rise in the population of GS pyrene aggregates, leading to a 5-fold increase in the I_E/I_M ratio as observed by steady-state fluorescence spectroscopy. This is shown in Figure 3.

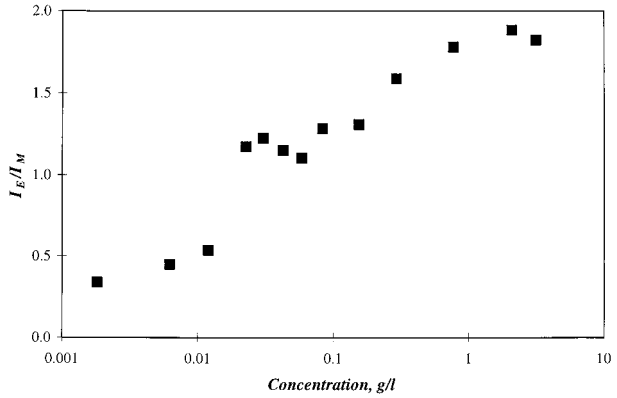

Figure 3. Plot of the ratios I_E/I_M versus polymer concentration in hexane with $\lambda_{ex} = 344$ nm. Calculation of the fluorescence intensities I_M and I_E is given in the Experimental Section.

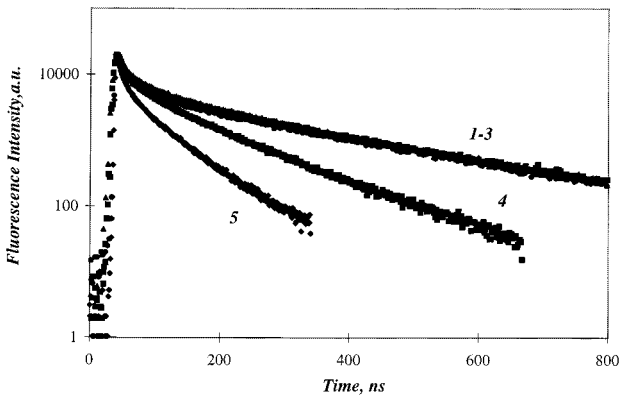

Figure 4. Fluorescence decays of the pyrene monomer ($\lambda_{ex} = 344$ nm; $\lambda_{em} = 377$ nm) of Py-EP*g*MA solutions in hexane: (1)−(5) [Poly] = 0.006, 0.040, 2.24, 43.6, and 178 g/L.

Fluorescence decay measurements were carried out for the pyrene monomer ($\lambda_{ex} = 344$ nm and $\lambda_{em} = 377$ nm). Such measurements yield information about the local environment probed by the pyrene monomer. We have seen in the Introduction that two processes lead to quenching of the pyrene monomers. They are depicted in Scheme 1. Process 1 corresponds to excimer formation within a GS pyrene aggregate. It occurs on a fast time scale due to the high local concentration of the pyrene groups. Process 2 describes the diffusional encounter between an excited single pyrene and either a GS unassociated pyrene or a GS pyrene aggregate. Process 2 occurs on a slow time scale. Figure 4 shows the fluorescence decays of the pyrene monomer obtained for several polymer concentrations. All decays exhibit some general features. A sharp peak is present at the early times. This corresponds to a process occurring on a fast time scale that we associate with process 1. At longer times, a long decay component is observed which we attribute to process 2. The presence of this long decay component is a clear indication that not all pyrene groups are associated into pyrene aggregates.

The fluorescence decays were first fitted with increasing numbers of exponentials. The longest decay time was fixed to the lifetime (τ_M) of an isolated pyrene attached onto the EP copolymer in hexane. τ_M was determined by monitoring the fluorescence decays of a pyrene labeled EP copolymer with a lower level of grafting (5×10^{-5} mol of pyrene per gram of polymer) to boost the emission from isolated pyrenes. τ_M was found to equal 260 ns. To obtain reasonable fits, a

Table 1. Parameters Obtained from Analysis of the Fluorescence Decays of the Pyrene Monomer with Four Exponentials (λ_{ex} = 344 nm and λ_{em} = 377 nm)

[Poly] (g/L)	A_1	τ_1 (ns)	A_2	τ_2 (ns)	A_3	τ_3 (ns)	A_4	τ_4 (ns)	χ^2
178	0.55	2.8	0.27	13.2	0.18	55	0.00	260	1.14
130	0.59	5.4	0.23	25.8	0.18	97	0.00	260	1.31
43.6	0.60	5.9	0.21	28.1	0.19	105	0.00	260	1.07
15.7	0.61	5.6	0.21	30.5	0.14	151	0.04	260	1.14
8.3	0.66	5.0	0.19	29.7	0.10	152	0.05	260	1.08
5.9	0.70	6.5	0.18	42.1	0.11	182	0.01	260	1.37
0.74	0.64	3.8	0.20	20.7	0.08	107	0.08	260	1.09
0.15	0.57	3.5	0.25	17.6	0.08	94	0.11	260	1.13
0.040	0.60	3.1	0.22	17.3	0.08	86.3	0.11	260	1.08
0.030	0.59	4.4	0.22	20.8	0.08	102	0.11	260	1.10
0.010	0.50	5.3	0.20	24.2	0.09	95	0.22	260	0.95
0.006	0.50	4.3	0.27	16.5	0.10	81	0.13	260	1.09

minimum of four exponentials are required. The results of this analysis are given in Table 1. However, the high number of exponentials used in the analysis makes the understanding of the system difficult. We will first give a qualitative analysis of the fluorescence decays, followed in the Discussion section by a more detailed and quantitative analysis using a blob approach.

Interestingly all fluorescence decays measured with polymer concentrations ranging from 0.006 up to 10 g/L overlap perfectly. It is worth noting that, over this same concentration range, the steady-state fluorescence data exhibits a 5-fold increase in the ratio I_E/I_M. This increase has been attributed to the formation of intermolecular pyrene aggregates.[1a] However, the perfect overlap of the time-resolved fluorescence decays carried out on the pyrene monomer indicates that *no* change is taking place in the local environment probed by the pyrene monomers. This local environment is made of the GS pyrene aggregates and the GS unassociated pyrene molecules which are the species able to quench pyrene fluorescence. Since the fluorescence decays overlap, this means that the local quencher concentration does not change in this polymer concentration range. This leads to the important conclusion that as the polymer concentration increases and more polar interactions are being generated, the composition of the polymer aggregate remains unchanged, keeping the local concentration of polar aggregates constant.

For polymer concentrations larger than 10 g/L, the long decay component shortens. This indicates that the local quencher concentration increases. The polymer concentration for which the long decay component starts to shorten is taken as the overlap concentration c^* of the polymer aggregates. According to our time-resolved fluorescence measurements, c^* occurs between 10 and 20 g/L. This is in qualitative agreement with the c^* calculated from the intrinsic viscosity $[\eta]$ of Py−EP*g*MA in hexane. We found that $[\eta]$ equals 0.038 L/g, leading to $c^* = [\eta]^{-1} = 26$ g/L.

Our time-resolved fluorescence measurements show that, as the polymer concentration is increased, the local concentration of polar aggregates remains constant throughout the polymer aggregates. This is possible only if either only a few polymer aggregates are present in the solution and they undergo outward growth or more polymer aggregates are being generated, both processes resulting in a constant concentration of polar junctions. At c^*, outward growth or polymer aggregate formation stops, and the polymer coils start to interpenetrate, forming an infinite polymeric network. This process is accompanied by an increase in the local concentration

Table 2. Parameters Obtained from Analysis of the Fluorescence Decays of the Pyrene Excimer with Three Exponentials (λ_{ex} = 344 nm and λ_{em} = 520 nm)

[Poly] (g/L)	A_1/A_2	A_2/A_2	A_3/A_2	τ_1 (ns)	τ_2 (ns)	τ_3 (ns)	χ^2
130	0.18	1.00	0.01	15.0	59.0	207	1.2
43.6*		1.00	0.18		53.6	95	1.2
15.7	−0.04	1.00	0.11	8.7	57.3	110	1.1
8.3	−0.06	1.00	0.11	6.8	56.7	103	0.9
5.9	−0.05	1.00	0.03	7.6	60.3	120	1.2
2.2	−0.08	1.00	0.03	11.8	60.2	162	1.1
0.74	−0.19	1.00	0.03	4.6	59.3	141	1.1
0.15	−0.18	1.00	0.01	7.5	62.8	184	1.1
0.040	−0.17	1.00	0.02	7.1	61.6	159	1.3
0.030	−0.24	1.00	0.13	9.3	58.5	95	1.0
0.010	−0.27	1.00	0.03	8.5	62.6	148	1.1

* The decay was fitted with two exponentials.

Table 3. Parameters Obtained from Analysis of the Fluorescence Decays of the Pyrene Monomer with Eq 4 (λ_{ex} = 344 nm and λ_{em} = 377 nm)

[Poly] (g/L)	f_{agg}	f_{diff}	f_{free}	$\langle n \rangle$	k_{agg} (10^8 s^{-1})	k_{diff} (10^7 s^{-1})	k_e[blob] (10^6 s^{-1})	τ_{free} (ns)	χ^2
178	0.51	0.46	0.03	1.7	3.4	3.6	14.0	103	1.11
130	0.53	0.38	0.00	1.7	2.8	3.0	9.0	125	1.27
44	0.59	0.30	0.11	2.0	1.7	1.6	6.5	126	1.07
16	0.57	0.32	0.12	1.8	2.0	2.1	4.5	207	1.10
8.3	0.60	0.29	0.10	1.8	2.3	2.3	4.5	226	1.05
2.2	0.69	0.20	0.11	2.2	2.1	1.6	4.3	222	1.32
0.74	0.60	0.28	0.12	1.7	1.8	2.1	5.2	250	1.06
0.15	0.55	0.34	0.12	1.7	2.3	2.6	3.3	266	1.13
0.04	0.56	0.30	0.14	1.7	1.8	2.0	3.6	265	1.06
0.03	0.58	0.28	0.13	1.8	1.9	2.2	4.0	257	1.08
0.01	0.54	0.28	0.18	1.4	1.8	1.6	4.1	272	0.95
0.006	0.55	0.33	0.12	1.8	2.4	2.7	3.9	264	1.09

of polar aggregates which results in the observed shortening of the fluorescence decays.

The excimer decays have been recorded for polymer concentrations ranging from 0.01 up to 130 g/L. Three exponentials were required to properly fit the excimer decays. The results of the fits are listed in Table 2. Although it was necessary to introduce a third exponential to obtain reasonable fits, its contribution to the decays was rather small ($A_3/A_2 < 0.13$). Due to its small contribution, the third decay time is retrieved with little accuracy. The third exponential is the longest component in the fluorescence decay, and it indicates a slow process of excimer formation, that we attribute to process 2 in Scheme 1. However, the small magnitude of the ratio A_3/A_2 leads to the conclusion that process 2 is not the dominant contributing factor in the excimer decays.

The second lifetime τ_2, which is associated with the heaviest preexponential weight, is always found to equal 60 ± 2 ns, a typical value for the pyrene excimer lifetime τ_E. For instance, the lifetime of the excimer of 1-pyrenylmethanamine has been reported to equal 64.5 ns.[13] Two polymer concentration domains can be defined. Below 15 g/L, the excimer shows a short rise time ($\tau_1 = 8.0 \pm 2.0$ ns) and a negative preexponential factor ($-1.0 < A_1/A_2 < 0.0$). Above 40 g/L, *no* rise time is observed. This behavior is shown in Figure 5 where the ratio A_1/A_2 is plotted as a function of polymer concentration.

When a system capable of forming excimers in liquids is well-behaved, the excimer decay can be fitted with a biexponential function. It exhibits a rise time that reflects the rate of production of the excimer. A steep rise time indicates an important excimer formation. Ideally, the ratio of the preexponential factors equals

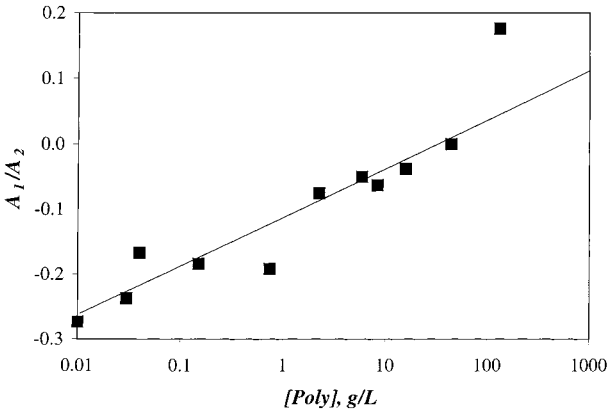

Figure 5. Plot of the ratios A_1/A_2 versus polymer concentration. A_1 and A_2 are obtained from the three exponential fit of the excimer decay ($\lambda_{ex} = 344$ nm; $\lambda_{em} = 520$ nm).

-1.0, according to the conventional Birks' scheme.[6] If ground-state dimers are present (such as the GS pyrene aggregates), the ratio A_1/A_2 takes a value that is more positive than -1.0. The more positive the A_1/A_2 value, the more ground-state dimers are present.

In all our excimer fluorescence decays, the ratios A_1/A_2 never equal -1.0, confirming the presence of a large population of GS pyrene aggregates. For polymer concentrations smaller than 40 g/L, the rise time (τ_1) is short, which indicates a high local concentration of pyrene groups, as could be the case inside a pyrene aggregate. As the polymer concentration is increased, the ratio A_1/A_2 increases steadily. This confirms the formation of additional intermolecular associations with increasing polymer concentration which is accompanied, above a polymer concentration of 15 g/L, by the observed shortening of the long component present in the fluorescence decay of the pyrene monomer. These associations generate the formation of more ground-state pyrene complexes which produce excimer instantaneously. This process is not resolved in the pyrene monomer fluorescence decay, a form of static quenching.

Because the kinetics of the monomer and the excimer are coupled, it is usually expected that any decay time observed in the decay of one population must be found in the decay of the other population. This is not clearly observed here (cf. Tables 1 and 2). Actually, none of the decay times shown in Table 1 can be observed in Table 2 and vice versa. This indicates that the kinetics are complicated and that a new approach must be found to investigate these experiments quantitatively. An effort to achieving this goal is presented in the Discussion section.

It is interesting to note that an earlier study[1a] has shown that an EP random copolymer grafted with maleic anhydride forms polymer aggregates in hexane. Dynamic light scattering measurements showed that these aggregates exhibit a constant size for polymer concentrations ranging from 0.3 up to 3 g/L.[1a] These results combined with the present study would lead to the suggestion that increased polymer concentration generates more polymer aggregates that would have the same size and the same polymer and polar junction composition, a process that would be reminiscent of micelle formation.

Discussion

As the investigated polymer system is fairly complicated and no treatment of excimer fluorescence of such systems has appeared in the literature, we needed to develop a model that is able to handle the measured fluorescence data and yield information about the polymer. Inspired by the success of the concept of blobs in handling complex polymer systems,[14] we adopted the approach of dividing the polymer network into an ensemble of blobs, as shown in Figure 6a. *A blob is defined as the volume probed by an excited pyrene having a lifetime* τ_0. The lifetime τ_0 is the longest decay component of an excited pyrene in the polymer network, and it is smaller than the natural lifetime of pyrene τ_M. Its expression will be discussed later. The polymer chains are held together via polyethylene crystallites and polar aggregates which are represented as smaller spheres. A more detailed view of a polar aggregate is shown in Figure 6b.

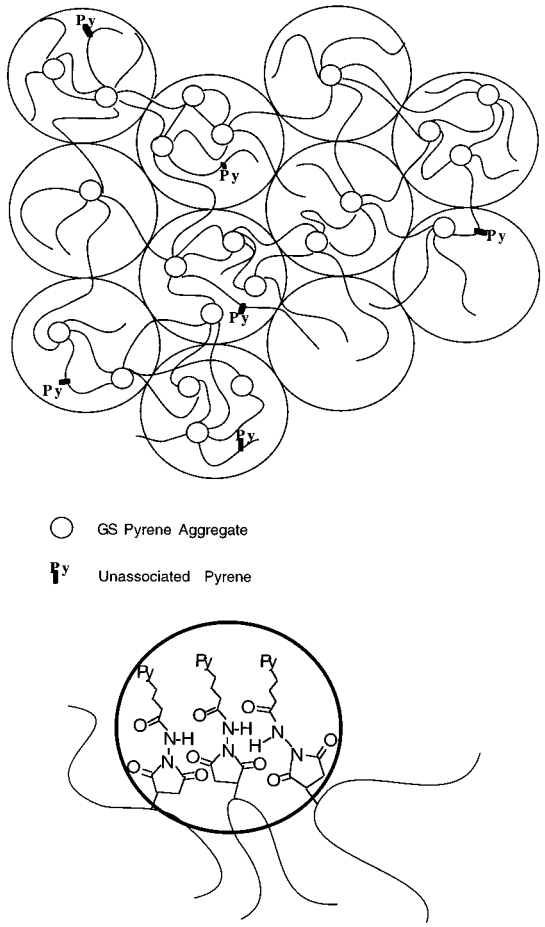

Figure 6. (a, top) Schematic view of a polymer network pictured as an ensemble of blobs. (b, bottom) Enlarged picture of a pyrene aggregate held in place by polar interactions between the succinic anhydride pendants.

During the lifetime τ_0 of an unassociated excited pyrene (Py^*_{diff}), Py^*_{diff} can either emit a photon or associate via diffusional encounter with a GS pyrene aggregate. Although Py^*_{diff} cannot leave a blob (a consequence of the definition of a blob), GS pyrene aggregates can diffuse in and out of the blobs. We show in the Appendix that the rate *f(t)* at which diffusional encounters between Py^*_{diff} and GS pyrene aggregates take place is a function of the average number $\langle n \rangle$ of GS pyrene aggregates inside a blob, the rate constant of exchange k_e of GS pyrene aggregates among blobs, the concentration of *blobs* within the polymer network [*blob*], and the rate constant for diffusional encounter

k_{diff} of one Py^*_{diff} and one GS pyrene aggregate inside one blob. When Py^*_{diff} has associated with a GS pyrene aggregate via polar interactions, the pyrene molecules rearrange rapidly within the aggregate to form an excimer with a rate constant k_{agg}.[7] k_{agg} has been presented in Scheme 1. According to Scheme 1 and the explanation below, the total fluorescence intensity of the pyrene monomer is the sum of three contributions:

$$[Py^*]_T(t) = [Py^*_{agg}](t) + [Py^*_{diff}](t) + [Py^*_{free}](t) \quad (3)$$

where $[Py^*_{agg}]$ is the concentration of excited pyrene monomers that are associated in a GS pyrene aggregate, $[Py^*_{diff}]$ is the concentration of excited pyrene monomer that are unassociated and can diffuse within the polymer network, and $[Py^*_{free}]$ is the concentration of a residual unquenched excited pyrene population which fluoresces with the natural lifetime of pyrene τ_M ($\tau_M > \tau_0$) at low polymer concentrations. An example of Py^*_{free} could be a single pyrene chromophore attached to a longer polymer chain that is not part of a polymer aggregate. The long polymer chain ensures the solubility of the pyrene labeled polymer and makes the association process between the polymer and the network less favorable. At low polymer concentrations, the excited pyrene fluoresces with its unquenched natural lifetime τ_M. Upon increasing the polymer concentration, encounters between Py^*_{free} and Py_{agg} present in the network occur more readily, resulting in the quenching of Py^*_{free} with a quenching rate constant k_{free}. Quenching of Py^*_{free} takes place in the same sequential manner depicted in Scheme 1 where the function $f(t)$ equals $k_{free}[Py_{agg}]$.[7b]

The expression for $[Py^*]_T(t)$ is derived in the Appendix according to Scheme 2. It is given in eq 4.

$$[Py^*]_T(t) = [Py^*_{agg}]_{(t=0)}e^{-(k_f+k_{agg})t} + [Py^*_{diff}]_{(t=0)}e^{-A_3}e^{-k_f t}\sum_{i=1}^{\infty}\frac{A_3^i}{i!} \times \left(\frac{A_2 + iA_4}{A_2 - k_{agg} + iA_4}e^{-k_{agg}t} - \frac{k_{agg}}{A_2 - k_{agg} + iA_4}e^{-(A_2+iA_4)t}\right) + [Py^*_{free}]_{(t=0)}(-k_{free}[Py_{agg}]e^{-k_{agg}t} + k_{agg}e^{-k_{free}t}) \times \frac{e^{-k_f t}}{k_{agg} - k_{free}[Py_{agg}]} \quad (4)$$

where $k_f = 1/\tau_M$ and the expression of A_2, A_3, and A_4 are given hereafter:

$$A_2 = \langle n\rangle \frac{k_{diff}k_e[blob]}{k_{diff} + k_e[blob]}, \quad A_3 = \langle n\rangle \frac{k_{diff}^2}{(k_{diff} + k_e[blob])^2}, \quad A_4 = k_{diff} + k_e[blob]$$

The longest decay time in eq 4 is due to the presence of pyrene groups unassociated with the polymer network (Py_{free}), and it equals $(k_{free}[Py_{agg}] + k_f)^{-1}$. It will be referred to as τ_{free}. The mole fractions f_{agg}, f_{diff}, and f_{free} of the three populations Py^*_{agg}, Py^*_{diff}, and Py^*_{free} are given in eq 5.

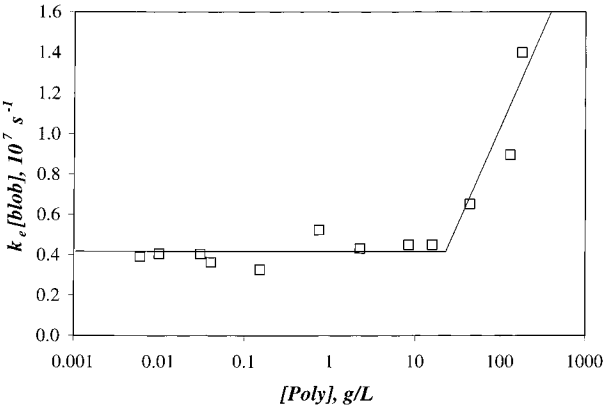

Figure 7. Plot of k_e[blob] versus polymer concentration.

$$f_{agg} = \frac{[Py^*_{agg}]}{[Py^*_{agg}] + [Py^*_{diff}] + [Py^*_{free}]}, \quad f_{diff} = \frac{[Py^*_{diff}]}{[Py^*_{agg}] + [Py^*_{diff}] + [Py^*_{free}]}, \quad f_{free} = \frac{[Py^*_{free}]}{[Py^*_{agg}] + [Py^*_{diff}] + [Py^*_{free}]} \quad (5)$$

Analysis of the fluorescence decays of the pyrene monomers according to eq 4 yields the mole fractions f_{agg}, f_{diff}, and f_{free}, the average number of GS pyrene aggregates $\langle n\rangle$ inside a blob, the rate constant k_{diff} for diffusional encounter between Py^*_{diff} and one GS pyrene aggregate inside a blob, the product k_e[blob] that characterizes the extent of exchange of GS pyrene aggregates among blobs, the rate constant k_{agg} for excimer formation within a GS pyrene aggregate, and the product $k_{free}[Py_{agg}]$ characterizing the quenching of pyrene groups attached to chains, which are not part of the polymeric network. For polymer concentrations below 1 g/L, all parameters remain constant. The longest decay time (τ_{free}) associated with Py_{free} equals 262 ± 8 ns. Since τ_M equals 260 ns, it indicates that for low polymer concentrations $[Py_{agg}]$ (which is the macroscopic concentration of the GS pyrene aggregates and is different from the local concentration of the GS pyrene aggregates inside the polymeric network $[Py^{loc}_{agg}]$) is rather small so that τ_{free} equals τ_M. The pyrene groups attached to polymers, which are not associated with the polymer network, are too far apart in the solution to combine with the polymer network on this time scale. For polymer concentrations larger than 1 g/L, τ_{free} decreases. This is a consequence of the increased pyrene concentration in the solution. For polymer concentrations below 15 g/L, all parameters describing the polymer aggregates remain constant with an average value and standard deviation given hereafter: $\langle n\rangle = 1.8 \pm 0.2$, $k_{diff} = (2.1 \pm 0.4) \times 10^7$ s^{-1}, k_e[blob] $= (4.2 \pm 0.6) \times 10^6$ s^{-1}, $k_{agg} = (2.1 \pm 0.2) \times 10^8$ s^{-1}, $f_{agg} = 0.57 \pm 0.05$, $f_{diff} = 0.31 \pm 0.04$, $f_{free} = 0.12 \pm 0.02$. We observe that the fastest rate constant is k_{agg} ($k_{agg} \gg k_{diff} \gg k_e$[blob]). Above 15 g/L, most parameters describing the pyrene aggregates remain constant, but k_e[blob] increases markedly as shown in Figure 7. This is a direct consequence of our predicted increase in the local

Table 4. τ_0 Values Calculated According to Eq 7 and the Parameters Listed in Table 3

[Poly] (g/L)	τ_0 (ns)
178	48
130	63
43.6	76
[Poly] < 16 g/L	101 ± 10

concentration of the GS pyrene aggregates ($[Py^{loc}_{agg}]$). Equation 6 gives the relationship between [blob] and $[Py^{loc}_{agg}]$.

$$[\text{blob}] = \frac{[Py^{loc}_{agg}]}{\langle n \rangle} \tag{6}$$

Since $\langle n \rangle$ remains constant within experimental error, an increase in $[Py^{loc}_{agg}]$ results in an increase in [blob], which is reflected in Figure 7. The increase in $[Py^{loc}_{agg}]$ leads also to the shortening of τ_0, the lifetime of an excited unassociated pyrene within the polymer network.

We have said earlier on that τ_0 does not equal τ_M, and the reason for this is now given. In Figure 6a, the polymeric network is divided into blobs, and the GS pyrene aggregates (the quenchers) are distributed randomly among the blobs. Figure 6a is very similar to that of a micellar system in which quenchers distribute themselves randomly among the micelles. If the quenchers are not able to leave and enter a micelle while a pyrene group remains excited, those micelles that contain one excited pyrene and *no* quencher will emit fluorescence with the natural lifetime of pyrene τ_M. In the case of the blob model, the quenchers are free to exit and enter the blobs. Thus, there is no empty volume in the polymer network where an excited pyrene can escape quenching by an incoming GS pyrene aggregate. The expression of τ_0 corresponds to the slowest decay rate of an excited pyrene located inside the polymeric network. It is obtained by setting $i = 0$ to the decay rate of the second exponential under the sum sign of eq 4. Its expression is given in eq 7.

$$\tau_0 = \left(\frac{1}{\tau_M} + \langle n \rangle \frac{k_{diff} k_e [\text{blob}]}{k_{diff} + k_e [\text{blob}]} \right)^{-1} \tag{7}$$

For concentrations smaller than 16 g/L, τ_0 takes an average value of 101 ± 10 ns. For polymer concentrations larger than 16 g/L, τ_0 has been calculated using the parameters recovered from the blob model analysis, and the values are listed in Table 4, indicating its decrease with increasing polymer concentration. Since the unassociated excited pyrene remains excited for a shorter period of time, it probes a smaller volume, and there is a decrease of the volume being probed by an unassociated excited pyrene, i.e., the blob volume. Since the blob volume (V_{blob}) decreases and $\langle n \rangle$ remains constant within experimental error, the local concentration of GS pyrene aggregates increases ($[Py_{agg}] = \langle n \rangle / V_{blob}$). This is in agreement with our previous conclusions.

As the polymer concentration is increased from the low concentration regime to the upper polymer concentration (178 g/L), τ_0 decreases 2.1 times. Assuming that the distance covered by diffusion motion is proportional to $(\tau_0/\eta)^{1/2}$, V_{blob} is proportional to the quantity $(\tau_0/\eta)^{3/2}$. The quantity η is referred to as the microviscosity[15] or the viscosity experienced locally by the pyrene groups located inside the polymer network. Consequently, as τ_0 decreases 2.1 times, one expects V_{blob} to decrease 3-fold, *keeping the microviscosity constant*. By definition (cf. Appendix), the rate constant, k_{diff} is the diffusional rate constant for encounter inside a blob containing an excited pyrene and one single GS pyrene aggregate. k_{diff} is inversely proportional to V_{blob}. As the blob volume decreases, reactants get closer, and one would expect k_{diff} to increase 3-fold as well. This is not observed experimentally (cf. Table 3). This means that the microviscosity increases with polymer concentration for polymer concentrations larger than 15 g/L.

The fraction of unquenched pyrene decreases with polymer concentration to reach barely detectable levels for the higher polymer concentrations ([Poly] > 140 g/L). As more and more aggregations are taking place, the volume not occupied by polymer aggregates decreases, until not enough free volume remains available for pyrene groups to remain unquenched.

We note that as k_{agg} tends to infinity (the normal mode of excimer formation with no GS pyrene aggregates), eq 4 reverts to eq A6.

In a recent article, some of us studied the dynamics of a PEO polymer in water, labeled with pyrene at specific positions.[7b] It was shown that the same Scheme 1 could be used to describe the association of the hydrophobic pyrene groups in water. k_{agg} was found to equal $(2.3 \pm 0.5) \times 10^8$ s^{-1}. This value agrees very well with that obtained for the modified EP copolymer studied in hexane, a completely different system.

The complexity of the system investigated in the present study requires the introduction of several parameters (k_{diff}, k_e[blob], $\langle n \rangle$, k_{agg}, f_{agg}, f_{diff}, f_{free}). It is clear that fitting our fluorescence decays with so many parameters may not have a unique interpretation, and the *blob* model analysis represents only one such interpretation of the data.

Conclusion

Fluorescence measurements have been carried out on a polymer labeled EP random copolymer grafted with maleic anhydride. They show that polar interactions are occurring between the maleic anhydride groups and that they mediate intermolecular polymer associations. Upon increasing polymer concentration, polymer aggregates form in which the concentration of the polar aggregates remains constant. Combining these results with those of a previous study[1a] leads to the suggestion that increasing polymer concentration could lead to the formation of an increased number of polymer aggregates of nearly constant sizes with unchanged polymer and polar junction composition, a process similar to micelle formation. As the overlap concentration is reached, interpenetration of the various polymeric aggregates takes place, inducing an increase of the local concentration of the polar junctions.

To quantitatively analyze our fluorescence decays, we describe the polymer aggregates as an ensemble of blobs into which GS pyrene aggregates are randomly distributed. The advantage of using a blob based approach is that the polydispersity of the system has no bearing on the analysis. The analysis now focuses on the characterization of a single blob. Although various concentration regimes were probed over the wide range of polymer concentrations studied (from 0.006 up to 178 g/L), the blob model analysis yielded good fits of the fluorescence

decays, and the system could be described quantitatively by a few parameters.

Acknowledgment. Jean Duhamel thanks NSERC, the University of Waterloo for start-up funds, and Imperial Oil for a University Research Grant.

Appendix

The pyrene labeled EP random copolymer system is viewed as a polymeric network held together by ordered domains of polyethylene sequences and polar aggregates. The polymer network is partitioned into blobs in which pyrene aggregates distribute randomly according to a Poisson distribution.[8] The pyrene aggregates account for most of the pyrene groups. The blobs are defined as the volume probed by an excited pyrene during its lifetime inside the polymeric network (τ_0 with $\tau_M > \tau_0$, see Discussion section, eq 6). The pyrene aggregates can diffuse in and out of the blobs. These processes are listed in eqs A1−A4:

fluorescence:

$$Py^*_{diff,n} \rightarrow Py_{diff,n} \quad 1/\tau_M \tag{A1}$$

exchange:

$$Py^*_{diff,n} + Py_{diff,j} \rightarrow Py^*_{diff,n+1} + Py_{diff,j-1} \quad jk_e Py^*_{diff,n} Py_{diff,j} \tag{A2}$$

exchange:

$$Py^*_{diff,n} + Py_{diff,j} \rightarrow Py^*_{diff,n-1} + Py_{diff,j+1} \quad nk_e Py^*_{diff,n} Py_{diff,j} \tag{A3}$$

aggregation:

$$Py^*_{diff,n} \rightarrow Py^*_{agg} \quad nk_{diff} \tag{A4}$$

where $Py^*_{diff,n}$ is the number of blobs containing one excited pyrene and n GS pyrene aggregates, $Py_{diff,j}$ is the number of blobs containing j GS pyrene aggregates, k_e is the rate of exchange of pyrene aggregate among blobs, and k_{diff} is the diffusion-controlled rate of encounter inside a blob containing one excited pyrene and one GS pyrene aggregate. These equations are adapted from those that were derived for micellar systems.[16] According to the classic mathematical derivation of Tachiya,[17] one obtains eq A5 as the time-dependent concentration profile of free excited pyrene disappearing via association with a pyrene aggregate.

$$[Py^*_{diff}](t) = [Py^*_{diff}]_{(t=0)} \exp(-(k_f + A_2)t - A_3[1 - \exp(-A_4 t)]) \tag{A5}$$

where the constants A_i are given hereafter:

$$A_2 = \langle n \rangle \frac{k_{diff} k_e [blob]}{k_{diff} + k_e [blob]}, \quad A_3 = \langle n \rangle \frac{k_{diff}^2}{(k_{diff} + k_e [blob])^2}, \quad A_4 = k_{diff} + k_e [blob]$$

Scheme 2

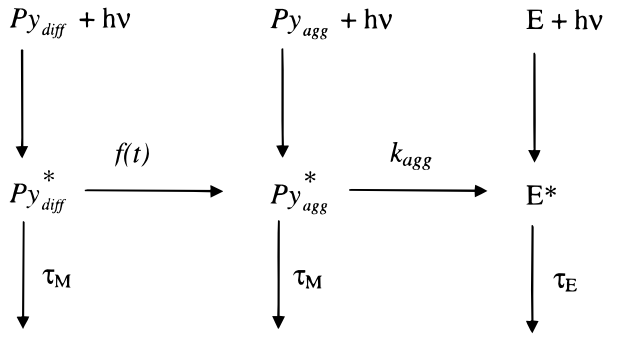

with [blob] being the local concentration of *blobs* inside the polymeric network and $\langle n \rangle$ being the average number of pyrene aggregates inside the *blobs*.

Once inside a pyrene aggregate, the pyrene groups rearrange to form an excimer at a high rate called k_{agg}, according to Scheme 2, where $f(t)$ is the rate of association and equals $-(d[Py^*_{diff}]/dt + k_f[Py^*_{diff}])$, and $[Py^*_{diff}]_{(t)}$ is given in eq A5. Equation A5 was then rewritten into a serial form

$$[Py^*_{diff}]_{(t)} = [Py^*_{diff}]_{(t=0)} e^{-A_3} \sum_{i=0}^{\infty} \exp[-(k_f + A_2 + iA_4)t] \frac{A_3^i}{i!} \tag{A6}$$

so that

$$f(t) = [Py^*_{diff}]_{(t=0)} e^{-A_3} \sum_{i=0}^{\infty} (A_2 + iA_4) \exp[-(k_f + A_2 + iA_4)t] \frac{A_3^i}{i!} \tag{A7}$$

From Scheme 2, we obtain the differential equation that describes the time dependence of concentration of the pyrenes located inside the pyrene aggregates ($[Py^*_{agg}]$):

$$\frac{d[Py^*_{agg}]}{dt} = f(t) - (k_f + k_{agg})[Py^*_{agg}] \tag{A8}$$

Combining eqs A7 and A8 yields eq A9.

$$[Py^*_{agg}] = [Py^*_{agg}] e^{-(k_f + k_{agg})t} + [Py^*_{diff}]_{(t=0)} e^{-A_3} \sum_{i=0}^{\infty} \frac{A_2 + iA_4}{A_2 - k_{agg} + iA_4} \frac{A_3^i}{i!} (e^{-(k_{agg} + k_f)t} - e^{-(A_2 + iA_4 + k_f)t}) \tag{A9}$$

so that the time-dependent profile of the total pyrene monomer concentration is given by eq A10.

$$[Py^*]_T(t) = [Py^*_{agg}](t) + [Py^*_{diff}](t) \tag{A10}$$

which yields

$$[\mathrm{Py}^*]_T(t) = [\mathrm{Py}^*_{\mathrm{agg}}]_{(t=0)}\mathrm{e}^{-(k_\mathrm{f}+k_{\mathrm{agg}})t} + [\mathrm{Py}^*_{\mathrm{diff}}]_{(t=0)}\mathrm{e}^{-A_3}\mathrm{e}^{-k_\mathrm{f}t}\sum_{i=0}^{\infty}\frac{A_3^i}{i!} \times \left(\frac{A_2 + iA_4}{A_2 - k_{\mathrm{agg}} + iA_4}\mathrm{e}^{-k_{\mathrm{agg}}t} - \frac{k_{\mathrm{agg}}}{A_2 - k_{\mathrm{agg}} + iA_4}\mathrm{e}^{-(A_2+iA_4)t}\right) \quad \text{(A11)}$$

For very large values of k_{agg}, we verify that eq A11 reverts to eqs A5 or A6.

It is also necessary to account for excited free pyrene groups which do not contribute to the polymeric network and fluoresce with their natural lifetime at low polymer concentration but undergo diffusional quenching at higher polymer concentrations according to Scheme 1. An expression to account for this additional quenching has been already derived in a previous paper[7b] and has been added to eq A11 to yield eq A12. These pyrene groups are referred to as $\mathrm{Py}^*_{\mathrm{free}}$, and the associated quenching rate constant is given as k_{free}.

$$[\mathrm{Py}^*]_T(t) = [\mathrm{Py}^*_{\mathrm{agg}}]_{(t=0)}\mathrm{e}^{-(k_\mathrm{f}+k_{\mathrm{agg}})t} + [\mathrm{Py}^*_{\mathrm{diff}}]_{(t=0)}\mathrm{e}^{-A_3}\mathrm{e}^{-k_\mathrm{f}t}\sum_{i=0}^{\infty}\frac{A_3^i}{i!} \times \left(\frac{A_2 + iA_4}{A_2 - k_{\mathrm{agg}} + iA_4}\mathrm{e}^{-k_{\mathrm{agg}}t} - \frac{k_{\mathrm{agg}}}{A_2 - k_{\mathrm{agg}} + iA_4}\mathrm{e}^{-(A_2+iA_4)t}\right) + [\mathrm{Py}^*_{\mathrm{free}}]_{(t=0)}(-k_{\mathrm{free}}[\mathrm{Py}_{\mathrm{agg}}]\mathrm{e}^{-k_{\mathrm{agg}}t} + k_{\mathrm{agg}}\mathrm{e}^{-k_{\mathrm{free}}t}) \times \frac{\mathrm{e}^{-k_\mathrm{f}t}}{k_{\mathrm{agg}} - k_{\mathrm{free}}[\mathrm{Py}_{\mathrm{agg}}]} \quad \text{(A12)}$$

The obtained equation appears complex, but it contains only relatively few variables, making the fitting procedure meaningful.

References and Notes

(1) (a) Nemeth, S.; Jao, T.-C.; Fendler, J. H. *Macromolecules* **1994**, *27*, 5449−5456. (b) Duhamel, J.; Yekta, A.; Hu, Y.; Winnik, M. A. *Macromolecules* **1992**, *25*, 7024−7030.
(2) Yekta, A.; Xu, B.; Duhamel, J.; Adiwidjaja, H.; Winnik, M. A. *Macromolecules* **1995**, *28*, 956−966.
(3) (a) Schulz, D. N.; Glass, J. E. Polymers as Rheology Modifiers. *ACS Symp. Ser.* **1989**, *No. 462*. (b) Glass, J. E. Polymers in Aqueous Media. *Adv. Chem. Ser.* **1989**, *No. 223*.
(4) Jao, T.-C.; Mishra, M. K.; Rubin, I. D.; Duhamel, J.; Winnik, M. A. *J. Polym. Sci., Part B: Polym. Phys.* **1995**, *33*, 1173−1181.
(5) Winnik, M. A. *Acc. Chem. Res.* **1985**, *18*, 73−79.
(6) Birks, J. B. *Photophysics of Aromatic Molecules*; Wiley: New York, 1970; pp 301−371.
(7) (a) Char, K.; Frank, C. W.; Gast, A. P. *Macromolecules* **1989**, *22*, 3177−3180. (b) Lee, S.; Duhamel, J. *Macromolecules* **1998**, *31*, 9193−9200.
(8) Duhamel, J.; Yekta, A.; Winnik, M. A.; Jao, T.-C.; Mishra, K.; Rubin, I. D. *J. Phys. Chem.* **1993**, *97*, 13708−13712.
(9) van Stam, J.; De Schryver, F. C.; Boens, N. N.; Herman, B.; Jerome, R.; Trossaert, G.; Goethals, E.; Schacht, E. *Macromolecules* **1997**, *30*, 5582−5590.
(10) Winnik, F. M. *Chem. Rev.* **1993**, *93*, 587−614.
(11) Demas, J. N. *Excited-State Lifetime Measurements*; Academic Press: New York, 1983; pp 102−111.
(12) Press, W. H.; Flannery, B. P.; Teukolsky, S. A.; Vetterling, W. T. *Numerical Receipes Fortran. The Art of Scientific Computing*; Cambridge University Press: New York, 1989; pp 523−528.
(13) Nemeth, S.; Jao, T.-C.; Fendler, J. H. *J. Photochem. Photobiol. A: Chem.* **1994**, *78*, 229−235.
(14) de Gennes, P.-G. *Scaling Concepts in Polymer Physics*; Cornell University Press: Ithaca, NY, 1979.
(15) Yekta, A.; Xu, B.; Duhamel, J.; Adiwidjaja, H.; Winnik, M. A. *Macromolecules* **1995**, *28*, 956−966.
(16) Dederen, J. C.; van der Auweraer, M.; De Schryver, F. C. *J. Phys. Chem.* **1981**, *85*, 1198−1202.
(17) Tachiya, M. *Chem. Phys. Lett.* **1975**, *33*, 289−292.

MA981129K